The Photometric Period of V392 Persei (Nova Persei 2018)

Richard E. Schmidt
Burleith Observatory, 1810 35th Street NW, Washington, DC 20007; schmidt.rich@gmail.com

Received January 25, 2020; revised March 10, 2020; accepted March 10, 2020

Abstract A photometric study of V392 Per (Nova Per 2018) has been undertaken at the urban Burleith Observatory in Washington, DC. A total of 1,010 CCD observations were obtained over a time span of 78.06 days. Analysis indicates an orbital period of 1.5841 h ± 0.0004 h, epoch (JD) of minimal light 2458839.52275, with amplitude 0.019 magnitude (Cousins I).

1. Introduction

The dwarf nova V392 Per (Nova Persei 2018), R.A. 04^h 43^m 21.37^s, Dec. +47° 21' 25.9" (2000), was first reported 50 years ago by Gerold A. Richter, Sonneberg Observatory, as a possible type U Gem variable of magnitude range 15–17 m_{pg} (Richter 1970). It was assigned type Z Cam (UGZ:) by (Liu and Hu 2000). Other catalogue names for this object are: S 10653, 2MASS J04432138+4721257, GSC2.3 NCFD013562, WISE J044321.38+472125.8. On 2018 April 29.4740 UT Yuji Nakamura, Kameyama, Japan, reported a magnitude 6.2 nova outburst (Nakamura 2018). Numerous follow-up observations confirmed this first thermonuclear eruption, which was accompanied by strong gamma-ray and X-ray emission (Murphy-Glaysher *et al.* 2019). The quiescent spectral energy distribution of V392 Per appears to rule out a red giant donor (Darnley and Starrfield 2018). The intensity of [NeV] 3426 neon lines suggests that this is an O-Ne-Mg white dwarf, or neon nova, as is Nova Cyg 1992 (Warner 2006; Munari and Ochner 2018). A preliminary orbital period was reported on 25 Jan. 2020 by (Schmidt 2020).

2. Observations

At Burleith Observatory, CCD observations were obtained with a 0.32-m PlaneWave CDK and SBIG STL-1001E CCD camera with an Astrodon Cousins I_c filter. This observatory is located in Washington, D. C., one of the brightest light polluted areas of the East Coast. In 2015 December, the sky background was measured as 18.50 ± 0.04 mag / arcsec^2 (I_c) (Schmidt 2016). From this location photometry in bands other than far-red optical is not feasible.

Prior to each night's run, the acquisition computer was synchronized to the USNO NTP time service. Images (240 sec, autoguided) were sky flat-fielded and dark corrected using The SKYX Professional Edition (Software Bisque 2020). An observing summary is given in Table 1.

3. Reductions

Synthetic aperture photometry was performed using MIRA PRO X64 version 8 (Mirametrics 2020). Aperture radii in 1.95 arc-second pixels were: object, 4; inner sky, 8; outer sky, 15. The field star Gaia DR2 2543617458239086 08 lies 8.6 arc seconds (4.4 pixels) north of V392 Per. It is reportedly stable at m_I = 13.977, m_v = 14.970 (Munari *et al.* 2020; Henden *et al.* 2016). This star was removed from each image prior to measurement, using the interactive pixel repair function of the aperture photometry package (Figure 1).

Table 1. Observation log. Time are UTC, not corrected for light travel time.

MJD start	*MJD end*	*Hours*	*Number of Observations*
58839.53131	58839.77779	5.92	54
58846.50502	58846.66373	3.81	33
58850.54891	58850.75502	4.95	44
58855.48628	58855.73133	5.88	62
58857.48038	58857.70976	5.51	60
58861.48409	58861.56303	1.89	23
58865.48278	58865.68026	4.74	50
58868.50348	58868.70290	4.79	49
58869.47865	58869.70119	5.34	57
58870.48553	58870.72153	5.66	64
58871.48648	58871.55852	1.73	21
58882.53477	58882.64854	2.73	39
58888.47759	58888.66063	4.39	59
58894.48230	58894.66850	4.47	63
58897.48101	58897.64268	3.88	46
58899.48560	58899.63067	3.48	48
58901.48301	58901.65186	4.05	51
58902.49476	58902.63006	3.25	37
58907.48439	58907.63131	3.53	49
58910.48860	58910.59473	2.55	38
58916.49398	58916.58354	2.15	32
58917.49434	58917.59207	2.35	31

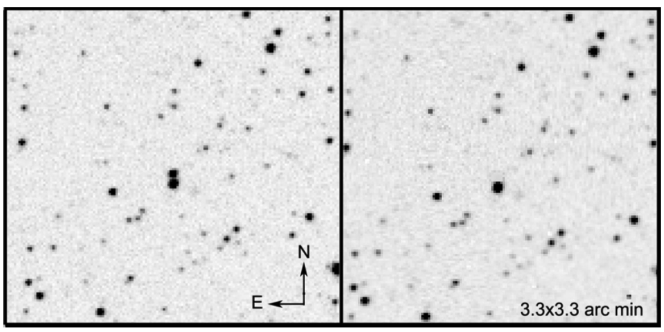

Figure 1. Removal of close field star.

Cousins I-band differential ensemble photometry was performed using the comparison stars from AAVSO chart sequence X24928QD (Table 2; C = comparison, K = check, Label = chart label).

The resulting magnitudes of V392 Per were detrended by subtracting the nightly means in order to remove the long-term

Table 2. Comparison stars.

AUID	R.A. (2000) h m s	Dec. (2000) ° ′ ″	C/K	Label	I_c	Mag. Error
000-BMQ-811	04 43 59.51	+47 24 18.6	1	130	11.720	(0.085)
000-BBH-307	04 43 07.45	+47 26 08.4	2	132	12.219	(0.186)
000-BBH-320	04 43 27.65	+47 25 49.4	3	135	12.421	(0.083)
000-BBH-306	04 43 04.85	+47 24 20.9	K	139	12.916	(0.161)

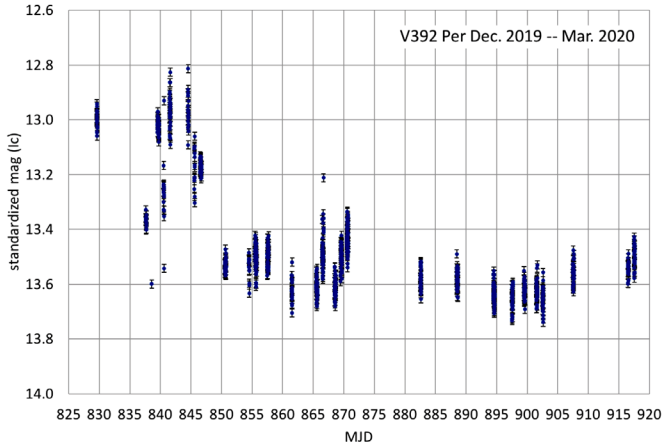

Figure 2. Observed I_c magnitudes, Dec. 2019–Mar. 2020.

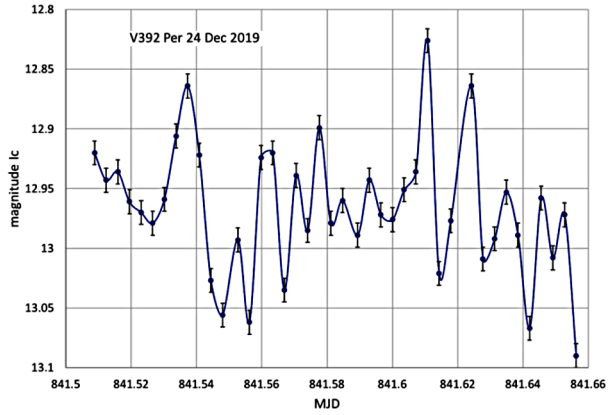

Figure 3a. Example session, 24 Dec. 2019.

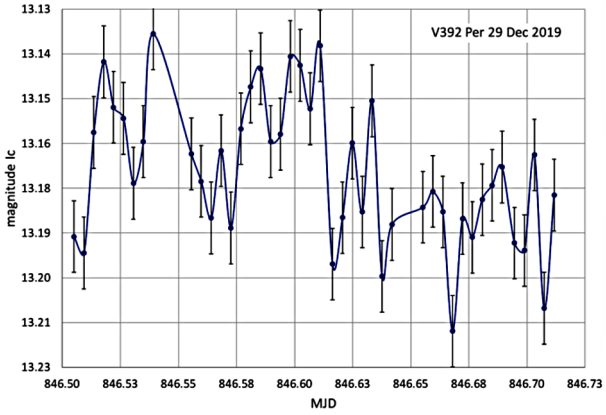

Figure 3b. Example session, 29 Dec. 2019.

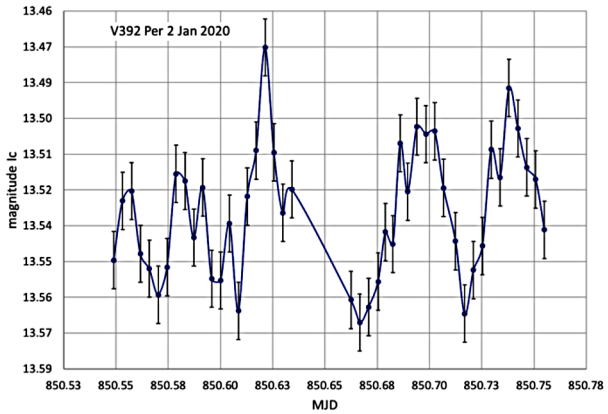

Figure 3c. Example session, 2 Jan. 2020.

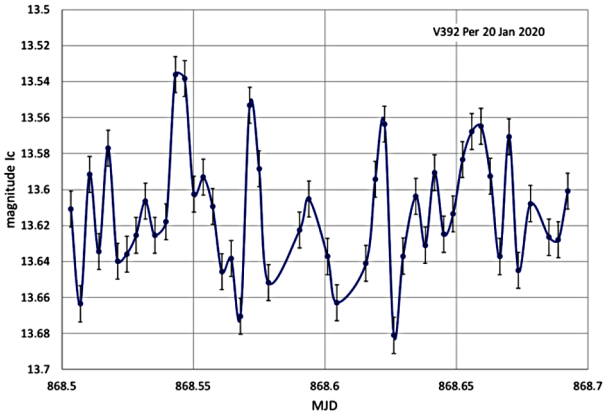

Figure 3d. Example session, 20 Jan. 2020.

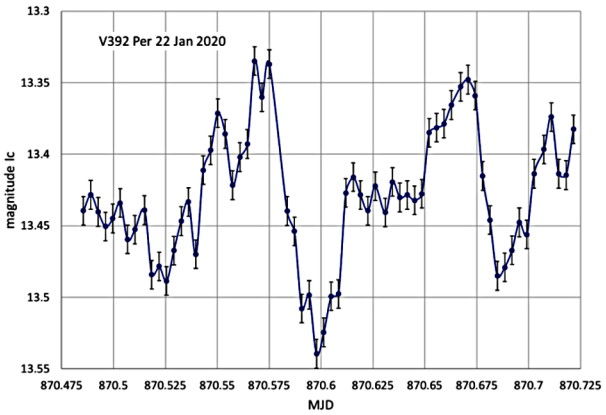

Figure 3e. Example session, 22 Jan. 2020.

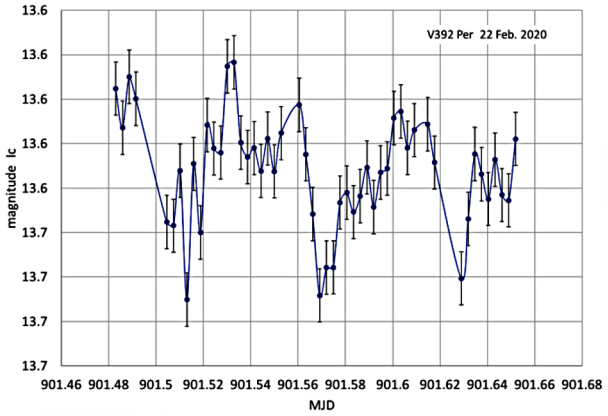

Figure 3f. Example session, 22 Feb. 2020.

light curve. Nightly observations, including unused sessions, are shown in Figure 2. Example observing sessions are shown in Figure 3.

4. Analysis

Period analysis of reduced-by-mean observations was performed using PERANSO 2.60 software (Vannmuster 2006). Using in turn both date-compensated discrete Fourier transform and Lomb-Scargle periodogram analyses, each gave the resulting period 1.5841 h ± 0.0004. Note that the error is a formal error of solution only, and not an indicator of the probability of reality of the observed period. The Lomb-Scargle periodogram is shown in Figure 4. Window aliases appear at about a frequency of 10 cycles per day (see VanderPlas 2018).

The most prominent period, 15.15 c / d, appears also in the minimum of the phase dispersion minimization (PDM) spectrum (Stellingwerf 1978), shown in Figure 5.

The most prominent period, 15.15 c / d, is shown in the folded double phase plot (Figure 6). A 225-point average with 128-point spline interpolation is shown (solid line), with amplitude 0.018 magnitude I_c.

The period was tested for significance using the PERANSO Fisher Monte Carlo randomization method which, while keeping observation times fixed, randomized the order of the magnitude observations over 200 permutations, searching for spectral responses due solely to observational biases (Moir 1998). The results were 0.005 ± 0.005 probability that no period was present in the data, and zero probability that any other significant periods were present in the data. The spectral window for all observations is shown in Figure 7. At frequency 15.15 cycles/day (dashed line), no spurious power appears, indicating that the period found is not due to the sampling frequency.

Table 3 summarizes the resulting period information.

5. Conclusion

The observed period of 95.05 minutes places Nova Persei 2018 squarely within the histogram of orbital periods of pre-cataclysmic variables found by (Nelson *et al.* 2018) and of the

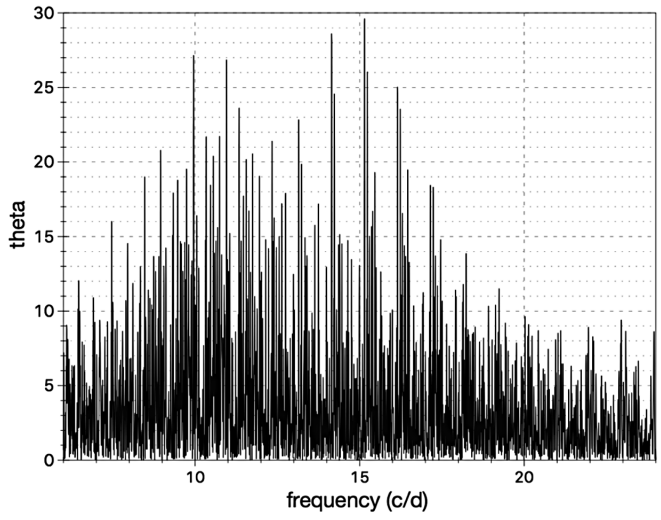

Figure 4. Lomb-Scargle periodogram.

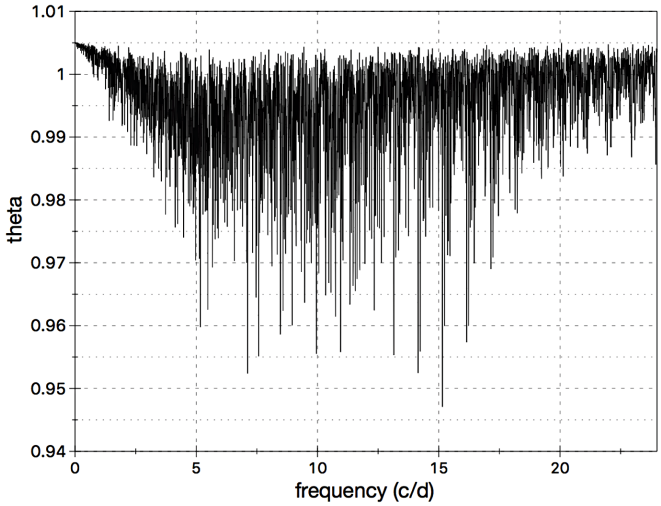

Figure 5. PDM spectrum.

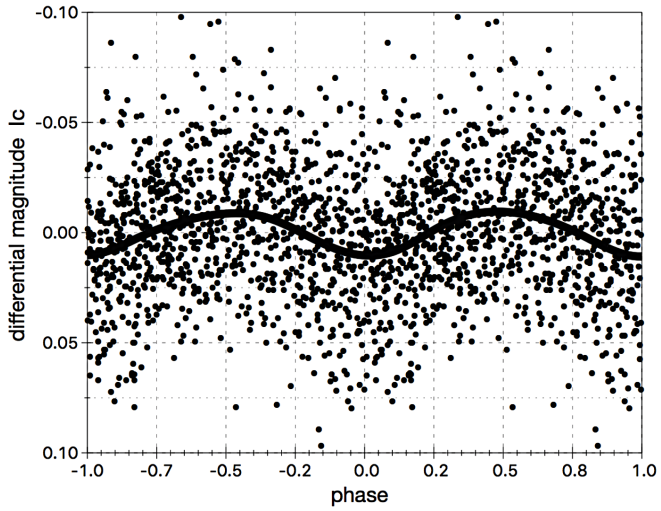

Figure 6. V392 Per, double phased plot with spline interpolated fit.

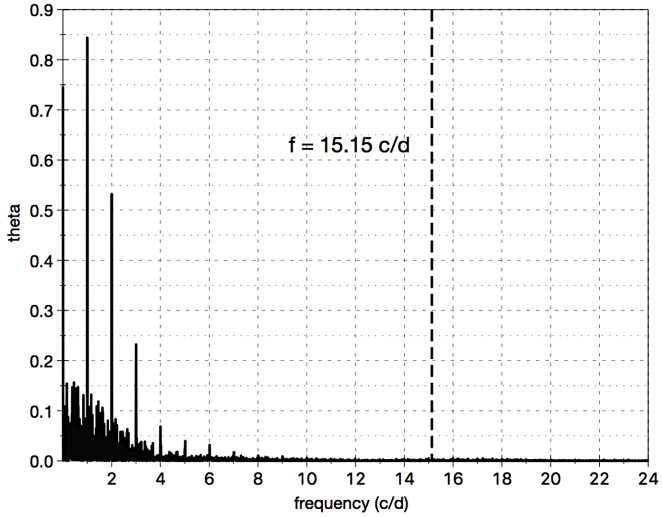

Figure 7. Spectral analysis for observational time aliases.

Table 3. Period analysis results for V392 Per.

Parameter	*Result*
Period(h)	1.5841 (0.0004)
Period(d)	0.06600 (0.00002)
Frequency(c/d)	15.15057 (0.0036)
Mean amplitude (fit)	0.019
Number of observations	1,010
Time span	78.0608 days
Epoch (JD) of minimum	2458839.52275

CVs found by the Sloan Digital Sky Survey (Southworth *et al.* 2012). V392 Per shows strong night-to-night flickering typical of cataclysmic variables, and this contributes much noise to the observations. If the observed photometric period is indeed orbital rather than a superhump period, the mass of a nova's Roche-lobe-filling main sequence secondary (M_2) would be uniquely determined as approximately $M_2 / M_\odot = 0.065\, P^{5/4}$ (Bode and Evans 2008).

For V392 Persei, $M_2 = 0.11\, M_\odot$. The orbital radius from Kepler's third law ("… it is absolutely certain and exact that the proportion between the periodic times of any two planets is precisely the sesquialterate [3/2] proportion of their mean distances…" (Kepler 1619)) for a primary mass of $1.2\, M_\odot$, for example, is 0.0034 AU, or about one-third that of the U Gem variable SS Cygni.

As was shown with Nova Cyg 1992 (V1974 Cyg), observations in Cousins I_c are effective in detecting photometric periodicity (DeYoung and Schmidt 1994), even near time of maximum. This implies that the nova shell may not be perfectly opaque in the red (Schaefer 2020). Further studies are warranted.

6. Acknowledgements

As modern astronomy stands upon the shoulders of giants, and of their supporting staff, we do well to pay tribute to the tireless observers of the Sonneberg Observatory's all-sky patrol which commenced in 1925 under C. Hoffmeister: G. A. Richter, Paul Ahnert, Nikolaus Richter, Johannes Hoppe, Sergej Gaposchkin, Heribert Schneller, Rudolf Brandt, Otto Morgenroth, Artur Teichgraeber, Hans Huth, and others. The author wishes to thank James A. DeYoung, NRL/USNO (ret.) for his invaluable advice. Special thanks to the AAVSO International Database for providing photometric standards for this study.

References

Bode, M., and Evans, A. 2008, *Classical Novae*, 2nd ed., Cambridge University Press, Cambridge, 25.

Darnley, M. J., and Starrfield, S. 2018, arXiv:1805.00994v2.

De Young, J. A., and Schmidt, R. E. 1994, *Astrophys. J., Lett.*, **431**, L47.

Henden, A. A., Templeton, M., Terrell, D., Smith, T. C., Levine, S., and Welch, D. 2016, AAVSO Photometric All Sky Survey (APASS) DR9, VizieR On-line Data Catalog II/336.

Kepler, J. 1619, *Harmonices Mundi*, Book V, Chapter III, Linz, Austria, Johannes Planck, 189–190.

Liu, W., and Hu, J. Y. 2000, *Astrophys. J., Suppl. Ser.*, **128**, 387.

Mirametrics, MIRA PRO X64 software, 2020 (http://www.mirametrics.com).

Moir, R. 1998, *Exp. Economics*, **1**, 87.

Munari, U., Moretti, S., and Maitan, A. 2020, *Astron. Telegram*, No. 13381, 1.

Munari, U., and Ochner, P. 2018, *Astron. Telegram*, No. 11926, 1.

Murphy-Glaysher, F. J., Darnley, M. J., Page, K. L. 2019, *Astron. Telegram*, No. 12951, 1.

Nakamura, Y. 2018, *Cent. Bur. Astron. Telegrams* "Transient Object Followup Reports," TCP J04432130+4721280 (www.cbat.eps.harvard.edu/unconf/followups/J04432130+4721280.html).

Nelson, L., Schwab, J., Ristic, M., and Rappaport, S. 2018, *Astrophys. J.*, **866**, 88.

Richter, G. A. 1970, *Mitt. Veränderl. Sterne*, **5**, 99.

Schaefer, B. E. 2020, private communication.

Schmidt, R. E. 2016, *Minor Planet Bull.*, **43**, 129.

Schmidt, R. E. 2020, IAU Circ., No. 4718, 1 (www.cbat.eps.harvard.edu/iau/cbet/004700/CBET004718.txt).

Software Bisque. 2020, THE SKY X Professional Edition (www.bisque.com).

Southworth, J., Gänsicke, B. T., and Breedt, E. 2012, in *Interacting Binaries to Exoplanets: Essential Modelling Tools*, eds. M. Richards, I. Hubeny, Proc. IAU Symp. 282, Cambridge University Press, Cambridge, 123.

Stellingwerf, R. F. 1978, *Astrophys. J.*, **224**, 953.

VanderPlas, J. T., 2018, *Astrophys. J., Suppl. Ser.*, **236**, 16.

Vannmuster, T., 2006, PERANSO period analysis software, v.2.60, CBA Belgium Observatory (http://www.cbabelgium.com/peranso).

Warner, B. 2006, *J. Amer. Assoc. Var. Star Obs.*, **35**, 98.